Study of Solvent Effects on the Fluorescence of 1-(Dimethylamino)-5-naphthalenesulfonic Acid and Related Compounds[1a]

Ying-Hsia Li,[1b] Lai-Man Chan,[1c] Linda Tyer, Robert T. Moody, Chester M. Himel,[1c] and David M. Hercules*

Contribution from the Departments of Chemistry and Entomology, University of Georgia, Athens, Georgia 30602. *Received April 23, 1974*

Abstract: The absorption and fluorescence spectra of 1-(dimethylamino)-5-naphthlenesulfonic acid, 1-(dimethylamino)-5-naphthalenesulfonamide, and 2-(dimethylamino)-6-naphthalenesulfonic acid and related compounds have been studied in different solvents. The fluorescence quantum yields and lifetimes in a variety of solvents as well as in binary solvent mixtures are reported. Highly polar solvents cause large red shifts in the fluorescence spectra of these compounds, particularly the 1-substituted aminonaphthalenes. The radiative rate constant for the 1-aminonaphthalenes decreases substantially with solvent polarity; the half-width of the fluorescence spectral band also is greater in polar solvents. These effects are not observed with 2-aminonaphthalene derivatives. The variations in fluorescence rate constant and bandwidth have been interpreted as arising from an inversion of the ^1L_a and ^1L_b excited states in 1-aminonaphthalenes. A mathematical model has been developed to describe the fluorescence behavior of 1-aminonaphthalenes in binary solvent mixtures based on the assumption of state mixing, the mixing coefficients determined by the solvent composition. The lowest electronic transitions of aminonaphthalenes involve mixing of the ^1L_a and ^1L_b states of naphthalene with a charge-transfer state arising from promotion of a lone-pair electron on the amino group into a π antibonding orbital of the ring. The resulting ^1L_a state is lowered in energy by approximately the amount of the ionization potential of the amino group, giving rise to a much smaller energy gap between the ^1L_a and ^1L_b states than in naphthalene. A change in configuration of the amino group from the ground state to the excited state enhances this effect. In 1-aminonaphthalenes, the ^1L_a state is polar, and the ^1L_b is nonpolar while, in 2-aminonaphthalenes, the ^1L_b is polar, and the ^1L_a state is nonpolar. In the 2-aminonaphthalenes, inversion of the excited states does not occur. No significant phosphorescence could be detected for any of the compounds studied in any solvent. Arguments are presented that intersystem crossing is relatively unimportant in these compounds. The transition moment was calculated for the 1,5- and 2,6-aminonaphthalenesulfonates in a variety of solvents. The results show that the transition moment of the 2,6 derivative is independent of solvent polarity, whereas the transition moments of the 1-amino derivatives show a sharp drop as the solvent polarity increases. This observation supports the concept of inversion of the excited states with increasing solvent polarity.

The use of substituted aminonaphthalenesulfonates as fluorescence probes in proteins and other macromolecules is well known.[2,3] These compounds show characteristic changes in the location of their fluorescence maxima and fluorescence intensity, which have permitted their use to determine "polar" and "nonpolar" sites in macromolecules. The anilinonaphthalenesulfonates (ANS derivatives) have been widely used with substitution in the 1 and 8 positions.[4,5] Another widely used probe has been 2,6-(*p*-toluyl)naphthalenesulfonate (TNS).[4,5] The only fluorescence probes having alkyl substituted amino groups are 1-(dimethylamino)-5-naphthalenesulfonate[6] (1,5-DNS) and its derivatives.

Both ANS and TNS derivatives have been studied using nanosecond time-resolved emission spectroscopy.[7,8] Solvent relaxation, mainly dipole reorientation,[7,9] and the variation of intersystem crossing yield[9,11] have been suggested as key factors responsible for variations in the fluorescence quantum yield of the probe molecules as a function of solvent. However, as will be shown below, these interpretations are not adequate to explain the 1,5-DNS system.

We were interested in defining the nature of the excited electronic state behavior of aminonaphthalenesulfonates as a function of solvent polarity. However, even for the simplest compounds having aryl groups on the nitrogen, the electronic transition of the aminonaphthalenes are highly complex; the lone electron pair on the nitrogen atom can be delocalized both in the phenyl and the naphthalene ring systems. We therefore chose to study the *N*-alkyl-substituted derivatives to avoid complications with the excited states of the benzene moiety.

We have observed a marked similarity between the solvent dependence of the fluorescence of 1,5-DNS and that of 1-(dimethylamino)naphthalene (1-DAN). This similarity has permitted use of simple naphthalene derivatives as models for the fluorescence behavior of 1,5-DNS. The low-energy excited states of aminonaphthalene derivatives have considerable charge-transfer character,[12,13] caused by mixing of the ^1L_a and ^1L_b states of naphthalene and the transition involving the lone-pair electrons on the nitrogen; this interaction results in a smaller energy separation between the ^1L_a and ^1L_b states than for naphthalene.[14,15] The nature of the lowest energy excited state in 1,5-DNS, i.e., the emitting state, is solvent dependent. In nonpolar solvents, fluorescence arises from the ^1L_b state of 1,5-DNS and, in polar solvents, from the ^1L_a state. In contrast, the emitting state for 2-(dimethylamino)-6-naphthalenesulfonate (2,6-DNA) is ^1L_b in both polar and nonpolar solvents.

Experimental Section

Chemicals. 1-(Dimethylamino)-5-naphthalenesulfonate (1,5-DNS) and 1-(dimethylamino)-5-naphthalenesulfonamide (1,5-DNSA) were synthesized and purified according to the method of Fussgänger.[16]

2-(Dimethylamino)-6-naphthalenesulfonate (2,6-DNS) (sodium salt) was obtained from Professor L. Brand of Johns Hopkins University; it was synthesized and purified by the procedure of Laurence.[17]

1-(Dimethylamino)naphthalene (1-DAN) (Eastman Organic Chemicals) was purified by vacuum distillation.

1-Naphthalenesulfonic acid (1-NSA) (Eastman Organic Chemicals) was purified by recrystallization from water.

1-Naphthalenesulfonamide (1-NSAA) was synthesized by warming 1-naphthalenesulfonyl chloride (Eastman Organic Chemicals) and concentrated aqueous ammonia solution for about 1 hr; the product was recrystallized twice from ethyl alcohol. The NMR spectrum of the product showed the presence of amide protons at δ 3.4 ppm.

Spectroquality *p*-dioxane, acetonitrile, benzene, methyl sulfoxide, formamide, and hexane were purchased from Matheson Coleman and Bell, spectrophotometric grade dimethylformamide from Mallinckrodt Chemical Co.

Both the Cary 14 and Cary 15 spectrophotometers were used to obtain absorption spectra. For quantum yield measurements, absorbance was in the range of 0.02–0.05 (1-cm path length) at the exciting wavelength. The actual measurement was done by using either a 5 or 10-cm path length quartz cell at room temperature; the fluorescence standards and sample solutions had equal absorbance at the exciting wavelength.

Room temperature fluorescence spectra were recorded on a G. K. Turner Associates Model 210 absolute spectrofluorometer. This instrument gives corrected emission and excitation spectra at constant energy. The relative quantum yields of fluorescence in various solvents were measured against that of 1,5-DNS in water (buffered with 0.1 *M* $NaHCO_3$, pH ~8.5); reported quantum yield is 0.36.[18,19] This experimental condition (pH ~8.5) was suggested by Chen[18] and appeared to be excellent. Quantum yield was independent of the presence of molecular oxygen. The effect of refractive index of each solvent on the quantum yield measurement is also corrected as suggested by Fletcher.[20]

A TRW Model 31 A nanosecond spectral source system and a Model 32 A decay-time analog computer plug-in module were used in conjunction with a dual-beam independent time base oscilloscope to measure fluorescence decay times.[21]

Phosphorescence spectra were recorded on an Aminco spectrophotofluorometer. The phosphorescence of 1,5-DNS in all solvents was checked by Professor J. D. Winefordner's laboratory at the University of Florida.

The calculations were done on computer by using "Basic" computer language, and all the results were plotted by an automatic plotter connected to the computer output.

Results

We have studied changes in the fluorescence spectra, absorption spectra, fluorescence lifetimes, and quantum yields as a function of solvent for 1-(dimethylamino)-5-naphthalenesulfonic acid (1,5-DNS) and amide (1,5-DNSA), 1-naphthalenesulfonic acid (1-NSA) and amide (1-NSAA), 1-(dimethylamino)naphthalene (1-DAN) and 2-(dimethylamino)-6-naphthalenesulfonic acid (2,6-DNS).

In order to diagnose the factors responsible for the solvent dependency of 1,5-DNS fluorescence, we have conducted identical studies on 1,5-DNS and 1,5-DNSA, as well as the three naphthalene derivatives directly related to these compounds, namely 1-NSA, 1-NSAA, and 1-DAN. The rationale behind this approach was to determine if one functional group in the naphthalene ring was responsible for the observed behavior, or if an interaction between the two groups was required.

Attempts to correlate fluorescence shifts with calculations involving dielectric constant and refractive-index values over a wide variety of solvents are usually unsuccessful. There are two empirical measures of solvent polarity in the literature: Kosower's *Z* value[22] and Dimroth's measure on transition energy $E_T(30)$.[23] These two parameters have been shown to correlate. For the present study we decided to treat solvent polarity as an empirical parameter and to adopt Dimroth's $E_T(30)$ as an indicator.

1-Naphthalenesulfonic Acid (1-NSA) and Amide (1-NSAA). The low-energy absorption maxima and the fluorescence maxima in a variety of solvents were plotted against $E_T(30)$ for 1-NSA, Figure 1, top, and 1-NSAA, Figure 2, top. It is evident that both absorption and fluorescence maxima for these compounds are invariant with solvent polarity.

The relative fluorescence quantum yields and lifetimes of 1-NSA, Figure 1, middle, and 1-NSAA, Figure 2, middle, were measured in two binary solvent mixtures: water–dioxane and acetonitrile–dioxane; the results are plotted against the percent dioxane. The ratios ϕ_x/ϕ_f and τ_x/τ_f are plotted in Figures 1 and 2, where ϕ_x and τ_x are the quantum yield and lifetime measurements at a given percentage of dioxane, and ϕ_f and τ_f are quantum yield and lifetime measurements in the pure polar solvent.

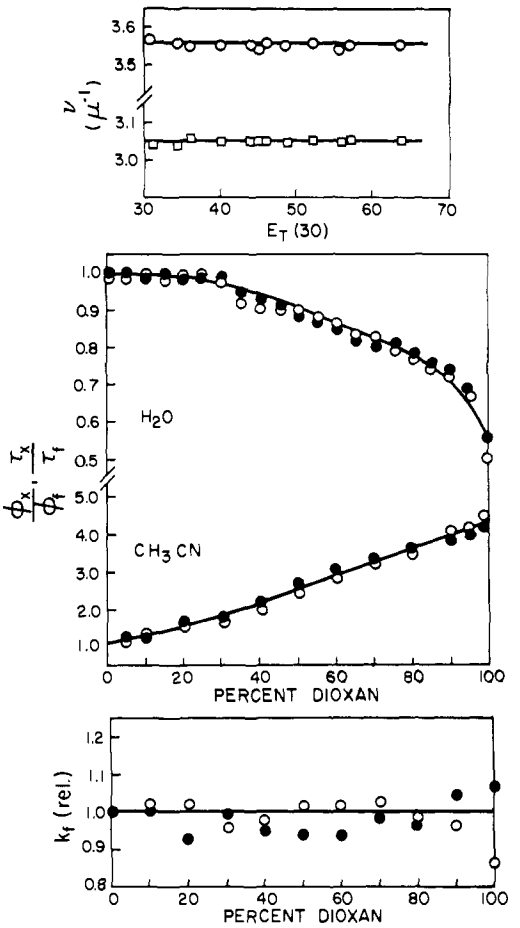

Figure 1. Spectral data for 1-naphthalenesulfonic acid (1-NSA). Top: frequency shifts with solvent polarity [(○) lowest energy absorption maximum; (□) fluorescence maximum]. Middle: quantum yields and fluorescence lifetimes in dioxane–water and dioxane–acetonitrile mixtures [(○) fluorescence quantum yield; (●) fluorescence lifetime]. Bottom: fluorescence rate constants in mixed solvent systems [(○) dioxane–water mixtures; (●) dioxane–acetonitrile mixtures].

Figures 1 and 2 indicate that the relative quantum yields and lifetimes for 1-NSA and 1-NSAA vary with solvent polarity. The ratio, $(\phi_x/\phi_f)/(\tau_x/\tau_f)$, which represents the relative fluorescence rate constant, k_f, is invariant with respect to solvent polarity.

The radiative rate constant for these compounds is estimated to be on the order of 5×10^7 sec^{-1}, which is an order of magnitude higher than that of naphthalene.

1-(Dimethylamino)naphthalene (1-DAN). The lowest energy absorption maximum shifts only slightly to the red as the solvent polarity increases, Figure 3, top. However, the fluorescence maximum shifts significantly to the red as the solvent polarity increases. Plots of relative fluorescence quantum yield and lifetime vs. percent dioxane are shown for 1-DAN in the middle of Figure 3. A striking difference is observed from similar plots for 1-NSA and 1-NSAA. In acetonitrile–dioxane mixtures, the relative fluorescence quantum yield and lifetime curves match well but, in water–dioxane mixtures, they differ. This difference results in a variation of fluorescence rate constant for water–dioxane mixtures, but not for acetonitrile–dioxane mixtures as seen in Figure 3, bottom. The absolute k_f value is in the range of $0.5–1 \times 10^8$ sec^{-1}.

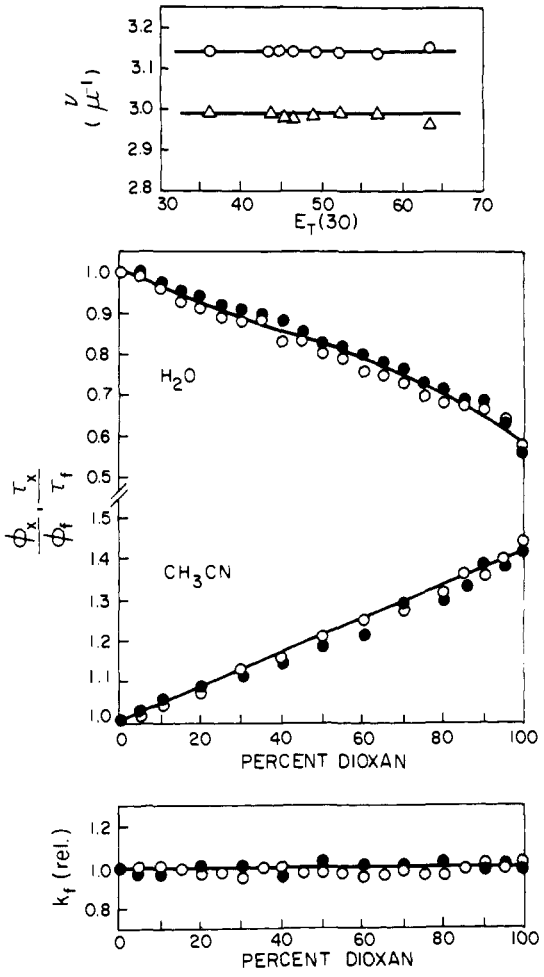

Figure 2. Spectral data for 1-naphthalenesulfonamide (1-NSAA). Top: frequency shifts with solvent polarity [(○) lowest energy absorption maximum; (△) fluorescence maximum]. Middle: quantum yields and fluorescence lifetimes in dioxane-water and dioxane-acetonitrile mixtures [(○) fluorescence quantum yield; (●) fluorescence lifetime]. Bottom: fluorescence rate constants in mixed solvent systems [(○) dioxane–water mixtures; (●) dioxane–acetonitrile mixtures].

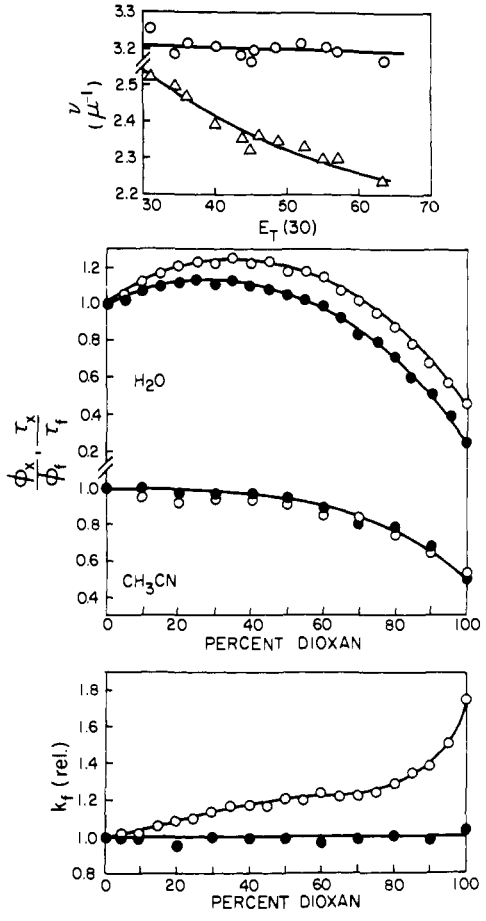

Figure 3. Spectral data for 1-(dimethylamino)naphthalene (1-DAN). Top: frequency shifts with solvent polarity [(○) lowest energy absorption maximum; (△) fluorescence maximum]. Middle: quantum yields and fluorescence lifetimes in dioxane-water and dioxane–acetonitrile mixtures [(○) fluorescence quantum yield; (●) fluorescence lifetime]. Bottom: fluorescence rate constants in mixed solvent systems [(○) dioxane-water mixtures; (●) dioxane–acetonitrile mixtures].

1-(Dimethylamino)-5-naphthalenesulfonic Acid (1,5-DNS) and Amide (1,5-DNSA). The plots of the lowest energy absorption maxima vs. $E_T(30)$ for both 1,5-DNS, Figure 4, top and 1,5-DNSA, Figure 5, top, show more scatter than for the other compounds studied; however, a straight-line fit through these points indicates no significant shift with increasing solvent polarity. Conversely, the fluorescence maxima of 1,5-DNS, Figure 4, top, and 1,5-DNSA, Figure 5, top, are highly sensitive to solvent polarity; as the solvent polarity increases, the energy of the fluorescence maximum decreases rapidly.

The relative fluorescence yields and fluorescence lifetimes of these two molecules in acetonitrile–dioxane and water–dioxane mixtures are shown in the middle of Figures 4 and 5. Figure 6, top, shows a similar plot for 1,5-DNS in 2-propanol–water mixtures. It is interesting that both molecules in each binary mixture behave similarly to 1-DAN in the water–dioxane mixture; i.e., the quantum yield and lifetime plots deviate significantly from each other. These curves may or may not have a maximum, and their maxima do not necessarily appear at identical solvent compositions. The relative k_f values are plotted vs. solvent composition at the bottom of Figures 4–6. The k_f values of 1,5-DNS and 1,5-DNSA decrease as the solvent polarity increases; the decrease is rather sharp for water–dioxane mixtures.

Examining the lowest energy absorption maxima of 1,5-DNS and 1,5-DNSA in binary solvent mixtures, one finds only slight solvent dependency as shown in Figure 7. Water is more effective in causing a blue shift than is acetonitrile. The fluorescence maxima of both compounds in acetonitrile–dioxane mixtures are sensitive to solvent polarity only at low concentrations of acetonitrile; most of the red shift occurs at acetonitrile concentrations below 10%. In dioxane–water mixtures, the fluorescence maximum shifts to the red drastically at water concentrations below 15%. Beyond that, the red shift is smaller but is still proportional to the water concentration. The red shift in water–dioxane mixtures is significantly greater than for acetonitrile–dioxane mixtures.

2-(Dimethylamino)-6-naphthalenesulfonic Acid (2,6-DNS). The absorption spectra of 2,6-DNS in various solvents show that the lowest energy absorption maximum does not shift significantly as the solvent polarity is changed, Figure 8, top. The fluorescence maximum shifts to the red as the solvent polarity increases. The magnitude of the shift in Figure 8, top, is about 2.0×10^3 cm^{-1}, significantly smaller than 3.0×10^3 cm^{-1} for 1-DAN, 3.2×10^3 cm^{-1} for 1,5-DNS, and 4.4×10^3 cm^{-1} for 1-DNSA.

Plots of ϕ_x/ϕ_f and τ_x/τ_f vs. solvent composition coincide for both the acetonitrile–dioxane and water–dioxane systems, Figure 8, middle. These results imply that solvent polarity essentially has no effect on the magnitude of k_f, as shown in Figure 8, bottom.

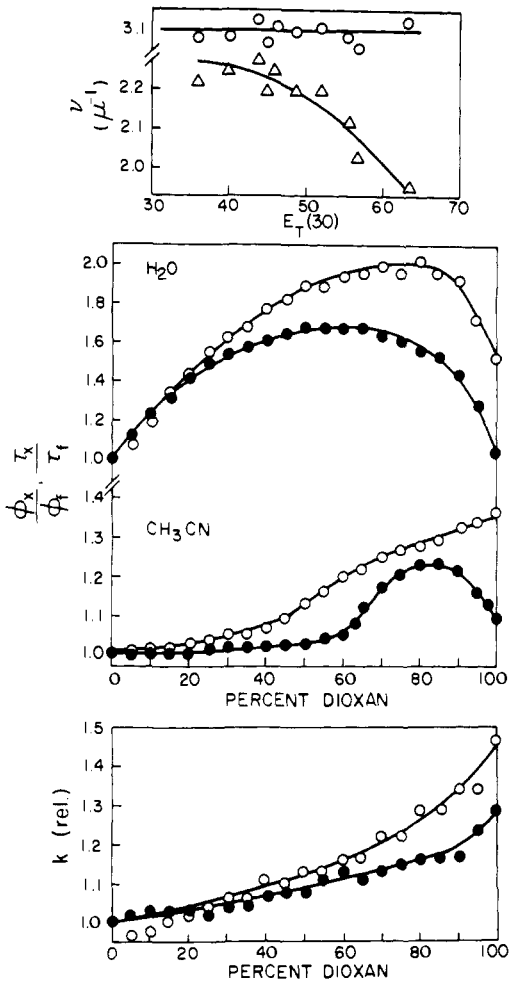

Figure 4. Spectral data for 1-(dimethylamino)-5-naphthalenesulfonic acid (1,5-DNS). Top: frequency shifts with solvent polarity [(○) lowest energy absorption maximum; (△) fluorescence maximum]. Middle: quantum yields and fluorescence lifetimes in dioxane-water and dioxane-acetonitrile mixtures [(○) fluorescence quantum yield; (●) fluorescence lifetime]. Bottom: fluorescence rate constants in mixed solvent systems [(○) dioxane–water mixtures; (●) dioxane–acetonitrile mixtures].

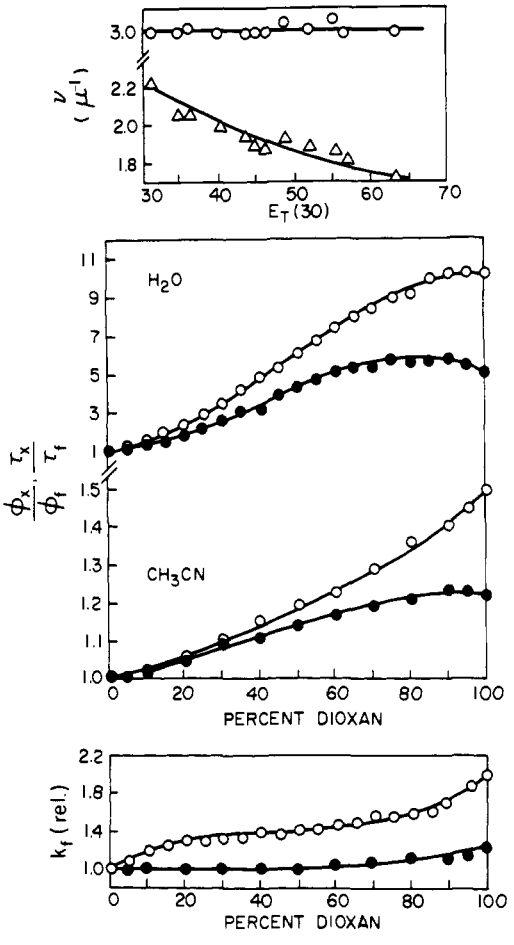

Figure 5. Spectral data for 1-(dimethylamino)-5-naphthalenesulfonamide (1,5-DNSA). Top: frequency shifts with solvent polarity [(○) lowest energy absorption maximum; (△) fluorescence maximum]. Middle: quantum yields and fluorescence lifetimes in dioxane–water and dioxane-acetonitrile mixtures [(○) fluorescence quantum yield; (●) fluorescence lifetime]. Bottom: fluorescence rate constants in mixed solvent systems [(○) dioxane–water mixtures; (●) dioxane-acetonitrile mixtures].

The corrected fluorescence quantum yields (18) and fluorescence lifetimes for 1,5-DNS, 1,5-DNSA, and 2,6-DNS were measured in a series of solvents and are listed in the order of increasing solvent polarity in Table I. These data indicate there is no systematic relationship between either $E_T(30)$ and ϕ_f or $E_T(30)$ and τ_f. Water seems to lower the fluorescence quantum yield of 1,5-DNS and 1,5-DNSA significantly, but not that of 2,6-DNS. Hexane seems to lower ϕ_f relative to other nonpolar solvents. However, this may be an artifact caused by low solubility.

In Table I, the most interesting feature is the variation of fluorescence rate constant with solvent. The values for k_f are plotted vs. $E_T(30)$ of the corresponding solvents in Figure 9; clearly there is a decrease with increasing solvent polarity. The slopes of the lines for 1,5-DNS and 1,5-DNSA are much greater than for 2,6-DNS. The k_f for the former two change by a factor of 2 or 3, whereas the total k_f change for 2,6-DNS is less than 20%. The shifts in the fluorescence maxima as a function of solvent for the three compounds (Figures 4, 5, and 8) show the same relative variations.

Phosphorescence of 1,5-DNS and 1,5-DNSA. No significant phosphorescence was detected for these two compounds on our Aminco instrument. We had these results

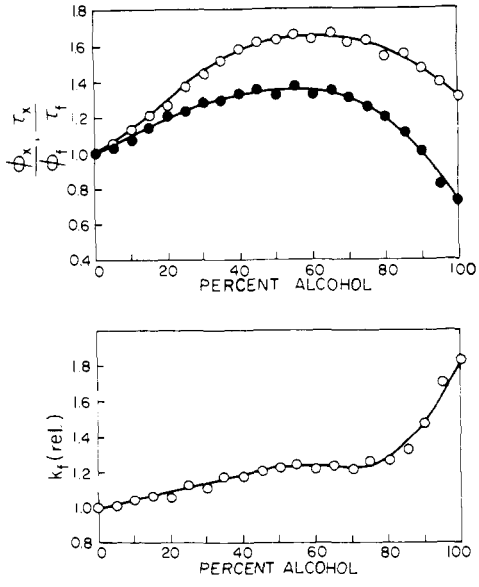

Figure 6. Spectral data for 1-(dimethylamino)-5-naphthalenesulfonic acid (1,5-DNS) in 2-propanol-water mixtures. Top: quantum yields and fluorescence lifetimes as a function of solvent composition [(○) fluorescence quantum yield; (●) fluorescence lifetime]. Bottom: fluorescence rate constant as a function of solvent composition.

Table I. Fluorescence Quantum Yields, Lifetimes, and Rate Constants for 1,5-DNS, 1,5-DNSA, and 2,6-DNS in Various Solvents

Solvent	Dielectric constant	$E_T(30)$, kcal/mol	Quantum yield (ϕ_f)			Lifetime (τ_f), nsec			Rate constant × 10^7 (k_f)		
			1,5-DNS	1,5-DNSA	2,6-DNS	1,5-DNS	1,5-DNSA	2,6-DNS	1,5-DNS	1,5-DNSA	2,6-DNS
Hexane[a]	1.890	30.9	0.19	0.31	0.39	4.3	8.1	6.9	4.42	3.83	5.65
Benzene[a]	2.284	34.5	0.51	0.55	0.45	10.1	13.3	7.8	5.05	4.14	5.77
Dioxane	2.209	36.0	0.58	0.60	0.64	11.8	17.8	11.4	4.92	3.37	5.61
DMF	37.50	43.8	0.54	0.53	0.70	11.9	19.1	12.3	4.54	2.78	5.69
DMSO	46.70	45.0	0.59	0.61	0.93	13.2	20.2	16.3	4.47	3.02	5.71
CH_3CN	37.50	46.0	0.38	0.37	0.49	9.2	14.6	9.3	4.13	2.53	5.26
2-Propanol	18.30	48.6	0.50	0.42	0.56	11.9	18.2	10.1	4.20	2.31	5.54
EtOH	24.30	51.9	0.46	0.39	0.54	12.9	17.1	10.2	3.57	2.22	5.29
Methanol	32.63	55.5	0.42	0.32	0.51	14.5	15.0	10.3	2.90	2.13	4.95
Formamide	109.5	56.6	0.48	0.37	0.46	17.5	16.4	8.8	2.74	2.26	5.23
Water	78.54	63.1	0.36	0.05[a]	0.88	16.5	3.3[a]	18.1	2.18	1.52[a]	4.86
D_2O	78.25		0.60	0.12[a]	0.93	26.7	8.4[a]	19.0	2.25	1.42[a]	4.89

[a] Compounds not sufficiently soluble in pure solvent. Values obtained by extrapolation of data in mixed solvents.

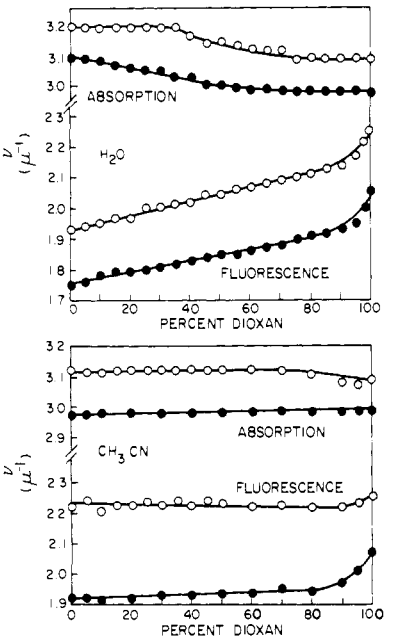

Figure 7. Effect of solvent composition on absorption and fluorescence maxima [(○) 1-(dimethylamino)-5-naphthalenesulfonic acid (1,5-DNS) (●) 1-(dimethylamino)-5-naphthalenesulfonamide (1,5-DNSA)]. Top: dioxane-water mixtures. Bottom: dioxane–acetonitrile mixtures.

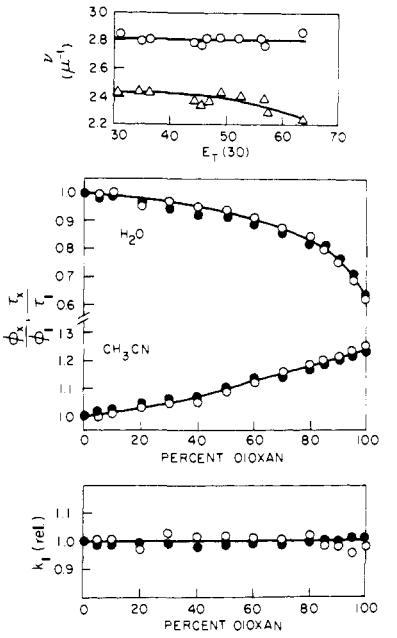

Figure 8. Spectral data for 2-(dimethylamino)-6-naphthalenesulfonic acid (2,6-DNS). Top: frequency shifts with solvent polarity [(○) lowest energy absorption maximum; (△) fluorescence maximum]. Middle: quantum yields and fluorescence lifetimes in dioxane-water and dioxane–acetonitrile mixtures [(○) fluorescence quantum yield; (●) fluorescence lifetime]. Bottom: fluorescence rate constants in mixed solvent systems [(○) dioxane–water mixtures; (●) dioxane-acetonitrile mixtures].

checked by Professor J. D. Winefordner's laboratory at the University of Florida using a more sensitive instrument. They could not detect any phosphorescence significantly higher than the solvent blanks. We have attempted to observe the triplet state of 1,5-DNS, using flash photolysis, without success. From these observations, we conclude that triplet states do not play a significant role in the excited-state processes of 1,5-DNS and 1,5-DNSA.

Discussion

In earlier studies,[7,9] the fluorescence behavior of ANS and TNS was interpreted on the basis of solvent relaxation effects. Recently, fluorescence behavior of ANS derivatives has been reported to arise from two excited states having different geometrical configurations.[24] The solvent relaxation explanation is inconsistent with our results, which have revealed that solvent effects on spectral shifts and variation of k_f values for 1,5-DNS and its derivatives are much larger than those of 2,6-DNS, despite the fact these two molecules have similar structure and size. Also, the low fluorescence quantum yield of 1,5-DNS in aqueous solutions cannot be

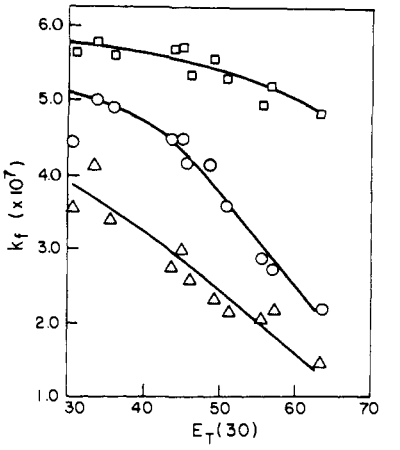

Figure 9. Fluorescence rate constants as a function of solvent polarity [(□) 2,6-DNS; (○) 1,5-DNS; (△) 1,5-DNSA].

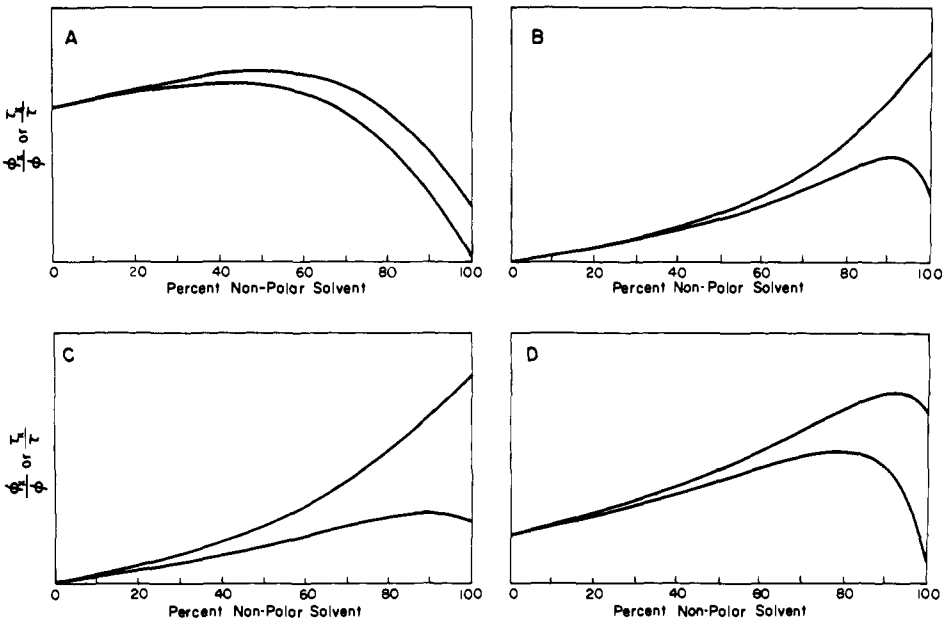

Figure 10. Calculated fluorescence quantum yields and fluorescence lifetimes in binary solvent mixtures: (upper curve) fluorescence quantum yield; (lower curve) fluorescence lifetime. (A) Input data: $f_n/f_p = 2.0$; $\gamma_n/f_p = 10.0$; $\gamma_p/f_p = 0.0$; $q_p/f_p = 2.0$; $K = 15$. (B) Input data: $f_n/f_p = 2.0$; $\gamma_n/f_p = 2.0$; $\gamma_p/f_p = 1.0$; $q_p/f_p = 5.0$; $K = 20$. (C) Input data: $f_n/f_p = 2.0$; $\gamma_n/f_p = 2.0$; $\gamma_p/f_p = 1.01$; $q_p/f_p = 5.0$; $K = 5$. (D) Input data: $f_n/f_p = 2.0$; $\gamma_n/f_p = 2.0$; $\gamma_p/f_\gamma = 0.5$; $q_p/f_p = 2.0$; $K = 20$.

explained by a large enhancement of intersystem crossing yield[9-11] since we were unable to detect any significant phosphorescence for these molecules in any solvent. Therefore there must be additional factors causing the effects observed for 1,5-DNS. The protonated species of 1,5-DNS can be formed in an excited-state proton-transfer reaction.[25] However, under our experimental conditions the aqueous solutions were neutral or slightly basic and many of our studies were done in aprotic solvent systems. This, coupled with the lack of spectral similarity to previous studies,[25] indicates that the results of the present study cannot be interpreted on the basis of excited-state equilibria. One can, on the other hand, devise a reasonable explanation for the experimental results assuming two emitting states of 1,5-DNS. We have devised a mathematical model which explains our experimental observations and is justifiable by the known excited-state behavior of the aminonaphthalenes.

Model for Excited-State Behavior. Assume there are two closely spaced excited states of a molecule, a polar one, P, and a nonpolar one, N. In a polar solvent, P is the emitting state and, in a nonpolar solvent, N emits. In a binary mixture of polar and nonpolar solvents, the emission observed will be from a composite of the two states:

$$S_x = \alpha_n(N) + \alpha_p(P)$$

where α represents the fractional contribution of each state to the composite state, S_x. The normalized coefficients α_n and α_p can be given by:

$$\alpha_n = \frac{S_n}{S_n + K(1 - S_n)}$$

$$\alpha_p = \frac{K(1 - S_n)}{S_n + K(1 - S_n)}$$

where S_p and S_n are the mole fractions of the polar and nonpolar solvents, respectively, and K is a constant, defining the solvent dependence of α_p and α_n.

If the composite state, S_x, is due to true mixing of two excited states, α_n and α_p will simply be the solvent-dependent mixing coefficients. Such a model naturally assumes only a small energy difference between N and P and neglects effects due to Jahn-Teller distortion. The model will be equally valid for two excited states having different geometries, as suggested by Kosower and Tanizawa,[24] for which K merely becomes the equilibrium constant for the solvent-dependent distribution between the two geometries.

For the situation involving excited-state mixing, the observed fluorescence rate constant for S_x will be a composite of the rate constant for the two individual states:

$$f_x = \alpha_n f_n + \alpha_p f_p$$

where f_p and f_n are the fluorescence rate constants of the polar and nonpolar states, respectively.

Similarly, the internal conversion ($S_1 \rightarrow S_0$) rate constant γ_x is

$$\gamma_x = \alpha_n \gamma_n + \alpha_p \gamma_p$$

where γ_p and γ_n are the internal-conversion rate constants for polar and nonpolar states, respectively.

If we assume that the polar solvent quenches fluorescence, the rate of quenching will be proportional to the concentration of polar solvent, therefore the pseudo-first order quenching rate constant is $q_p[S_p] = q_p(1 - S_n)$, where q_p is the quenching rate constant of the polar solvent.

Thus the total fluorescence decay time, τ_x in any given solvent mixture, can be written as:

$$\tau_x = \frac{1}{[f_x + \gamma_x + k_{isc} + q_p(1 - S_n)]} \quad (1)$$

and the fluorescence quantum yield is

$$\phi_x = f_x \tau_x \quad (2)$$

The intersystem crossing rate constant is assumed to be invariant with respect to x. It appears to be negligibly small in the compounds studied here and subsequently will be neglected.

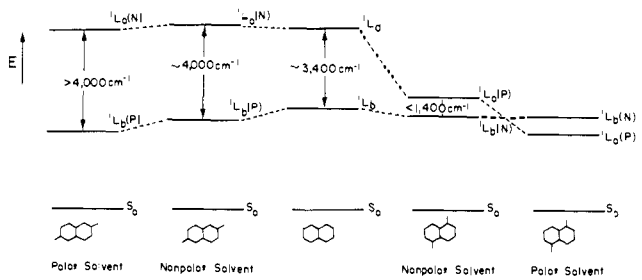

Figure 11. Solvent effects on the ^1L_a and ^1L_b transition energies for 1- and 2-aminonaphthalenes: P = polar state; N = nonpolar state.

Some sample calculations were performed using eq 1 and 2 to see if the model would qualitatively fit the data observed for 1,5-DNS and 1,5-DNSA. These calculations were done using various values for f_n, f_p, γ_n, γ_p, and K, assuming in all cases that the rate constant for intersystem crossing was zero. All calculations were done in terms of ratios of rate constants in order to avoid the necessity of establishing the absolute magnitudes of these values. The results of the calculations are shown in Figure 10. In all cases, fluorescence quantum-yield curve is the upper curve, and the fluorescence lifetime curve is the lower curve.

There is a striking resemblence between the curves generated in Figure 10 and the data obtained for 1,5-DNS and its derivatives experimentally. The calculated curves in Figure 10A are very similar to the behavior of 1-DAN in water–dioxane mixtures, shown in Figure 3. There is also considerable similarity between Figure 10B and the behavior of 1,5-DNS in acetonitrile–dioxane mixtures shown in Figure 4. Figure 10C clearly resembles the behavior of 1,5-DNSA in acetonitrile–dioxane mixtures shown in Figure 5. Figure 10D shows similarity to the behavior of 1,5-DNS in 2-propanol–water mixtures as shown in Figure 6.

Although the above comparison is only qualitative, the fact that curves of significantly different shapes can be generated simply by varying the parameters involved, and that these shapes match very closely the shapes of curves observed for the 1,5-DNS system, constitutes a strong argument that the model proposed has validity, and that 1,5-DNS and its derivatives have different emitting states in polar and nonpolar solvents.

Excited States of Aminonaphthalenes. Platt[26] has termed the two lowest $\pi \rightarrow \pi^*$ transitions for polyacenes as ^1L_a and ^1L_b. For naphthalene, the ^1L_b state is lower in energy than ^1L_a by about 3400 cm^{-1} and is long-axis polarized. The ^1L_b orbital wave functions have nodes between the β-carbon atoms and at the α-carbon atoms. The ^1L_a state is short-axis polarized, and its orbital wave functions have their nodes at the carbon atoms fusing the two rings and a large density on the α-carbon atoms.[27] Because of the difference in electron distribution in the two excited states, a substituent at the 1 position of naphthalene will interact more effectively with the ^1L_a excited state than with the ^1L_b state; conversely, 2-position substituents will interact more strongly with the ^1L_b state.

In aromatic systems, intramolecular charge-transfer transitions arise from mixing of the $\pi \rightarrow \pi^*$ transition of the aromatic ring with the lone-pair transition from the amino group, designated $l \rightarrow \pi^*$ by Kasha.[28] Such a mixed transition will occur in 1-aminonaphthalenes involving the ^1L_a transition of naphthalene and the lone pair of the amino group. The ^1L_b band of 1-aminonaphthalene has much less charge-transfer character and remains essentially a $\pi \rightarrow \pi^*$ transition. Conversely, in 2-aminonaphthalene, the ^1L_b band will acquire charge-transfer character, while the ^1L_a band will remain largely a $\pi \rightarrow \pi^*$ transition.

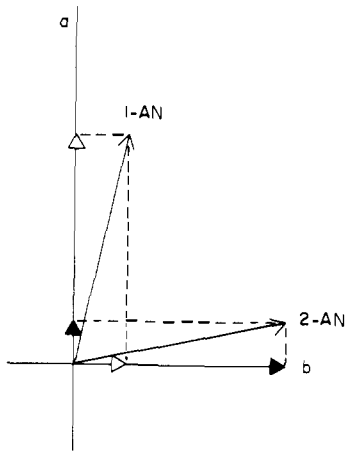

Figure 12. Vector model for aminonaphthalenes [(▲) 1-aminonaphthalene; (▶) 2-aminonaphthalene]. See text for explanation.

Nishimoto et al.[14,15] have done calculations on the electronic transitions of substituted naphthalenes. They predict that all transitions of 1-aminonaphthalene, in particular the ^1L_a transition, are shifted to the red relative to those of naphthalene. These shifts result in a smaller energy gap (~1400 cm^{-1}) between the ^1L_a and ^1L_b bands with ^1L_b still remaining as the lowest excited state. They also found the energy shifts of the $\pi \rightarrow \pi^*$ transition of 2-aminonaphthalene cause a larger energy gap between the ^1L_a and ^1L_b bands. This prediction is in agreement with the experimental observations of Brand et al.[13] These results are summarized in Figure 11 for 1-substituted aminonaphthalenes (right-hand side) and 2-substituted aminonaphthalenes (left-hand side).

The lowest energy absorption bands of the aminonaphthalene derivatives are relatively insensitive to solvent polarity, whereas the fluorescence spectra are highly solvent sensitive. This effect has been explained by the large increase in dipole moment (μ) upon excitation.[9] Mataga[29] suggested that the increase in dipole moment was caused by a change in the configuration of the amino group from tetrahedral (sp^3) in the ground state to trigonal (sp^2) in the equilibrium excited state, S_1. This suggestion has been applied by El-Bayonmi, et al.[30] to explain the anomalous difference between the observed and calculated fluorescence lifetimes of 2-aminonaphthalene. A similar idea has been used by Kosower and Tanizawa[24] to explain the fluorescence of 2-(*N*-arylamino)-6-naphthalenesulfonates.

Schulman and Capomacchia[31] have shown that the second absorption band (^1L_a) of 2-aminonaphthalene does not shift as much as the lowest absorption band (^1L_b) on protonation; the second band is not as sensitive to β substitution. They indicated that a change in the electronic configuration of the amino groups upon excitation may cause the ^1L_b state of 2-aminonaphthalene to be more polar than the ^1L_a state. These results are consistent with a simple vector analysis as shown in Figure 12.

The two vectors (**1-AN** and **2-AN**) correspond to the dipole changes of 1- and 2-aminonaphthalenes because of electronic-configuration changes of the amino group. The a and b axes are the short and long axis of naphthalene, respectively, i.e., the axes of the ^1L_a and ^1L_b transitions. The projection of the dipole change from 2-aminonaphthalene (solid arrows) is larger on the b axis than on the a axis. In the case of 1-aminonaphthalene, the situation is reversed (open arrows). Thus one can see that the ^1L_b transition of 2-aminonaphthalene has a larger dipole change than ^1L_a but, for 1-aminonaphthalenes, the converse is true. Therefore, for 1-aminonaphthalene, ^1L_a is the polar (P) state, and

^1L_b is the nonpolar (N) state; for 2-aminonaphthalene, ^1L_b is the polar (P) state, and ^1L_a is the nonpolar (N) state.

How these factors affect the relative energies of the excited states of the aminonaphthalenes is summarized in Figure 11. In 2,6-DNS (shown on the left), the major charge-transfer interaction will involve the ^1L_b state; thus it will be polar and lowered in energy relative to the ^1L_a state and to the ^1L_b state of naphthalene. In a polar solvent, the major polar interaction will lower the ^1L_b state further. Note, the ^1L_b state will be the emitting state both in polar and nonpolar solvents.

For 1,5-DNS (shown on the right), the main charge-transfer interaction involves the ^1L_a state, lowering it significantly relative to the ^1L_a state of naphthalene; the ^1L_b state of 1,5-DNS is close to that of naphthalene and only ca. 1400 cm^{-1} below the ^1L_a state. In a polar solvent, the major polar interaction will involve the ^1L_a state of 1,5-DNS and, if this interaction is sufficiently large, the ^1L_a state can have lower energy than the ^1L_b, as shown. This means that, in 1,5-DNS and similar compounds, solvent polarity will govern which is the emissive state. If the energies of the ^1L_a and ^1L_b states are nearly equal, state mixing will occur, and the emission characteristics observed would be a composite of those for the individual states. This is entirely consistent with the mathematical model proposed above, and with our experimental observations on 2,6-DNS and 1,5-DNS and its derivatives.

One difficulty in interpreting the data for 1,5-DNS is that we have no direct proof of the assumption that intersystem-crossing yield is either negligible or constant. The observation $\phi_p \simeq 0$ is a good indication that this is valid, but intersystem crossing, coupled with radiationless decay of the triplet, could also give $\phi_p = 0$. The nonradiative rate constant for 1,5-DNS is $(k_{nr})_{H_2O} = 3.88 \times 10^7$ sec^{-1} in water and $(k_{nr})_{D_2O} = 1.50 \times 10^7$ sec^{-1} in deuterium oxide; for 1,5-DNSA, $(k_{nr})_{H_2O} = 28.48 \times 10^7$ sec^{-1} in water, and $(k_{nr})_{D_2O} = 10.48 \times 10^7$ sec^{-1} in deuterium oxide, where $k_{nr} = k_{ic} + k_{isc} + q_p$. The intersystem crossing transition which is allowed through spin–orbit coupling should not be affected by solvent deuteration, and thus k_{isc} should be constant. The internal-conversion rate (k_{ic}) which depends on the magnitude of the energy gap and the Franck–Condon factor between the excited state and the ground state should also be insensitive to solvent deuteration. Therefore, the nonradiative transition is mainly caused by solute–solvent vibrational relaxation. The large difference in $(k_{nr})_{H_2O}$ and $(k_{nr})_{D_2O}$ is attributed to the difference in vibrational coupling of the O–H stretching modes and O–D stretching modes of water and deuterium oxide, respectively. Solvent relaxation has been treated as quenching by the polar solvent in our mathematical model. Therefore q_p, the polar solvent quenching factor, depends not only on the solvent polarity but also on its vibrational modes. Our conclusion is that $q_p > k_{isc}$, and that the latter can be neglected.

Mixing of States. Vibronic interaction always plays an important role, in terms of perturbation theory, in the mixing of two states. By applying the adiabatic approximation,[32] adiabatic wave functions of the perturbed electronic states can be written in terms of the vibrational nuclear displacement Q:

$$\Phi_1(Q) = \alpha(Q)\Psi(^1L_a) + \beta(Q)\Psi(^1L_b)$$

$$\Phi_2(Q) = -\beta(Q)\Psi(^1L_a) + \alpha(Q)\Psi(^1L_b)$$

where $\alpha(Q)$ and $\beta(Q)$ are normalized mixing coefficients. The radiative rate constant corresponding to these perturbed states would be either $(k_f)_1 = \alpha^2 k_f(^1L_a) + \beta^2 k_f(^1L_b)$ or $(k_f)_2 = \beta^2 k_f(^1L_a) + \alpha^2 k_f(^1L_b)$ depending upon which state is emitting. As ^1L_a and ^1L_b are degenerate or nearly degenerate $\alpha \simeq \beta \simeq 1/2$, $(k_f)_{1,2} = \frac{1}{2}k_f(^1L_a) + \frac{1}{2}k(^1L_b)$. This serves to explain why, when ^1L_a has shifted from just slightly above ^1L_b to just below ^1L_b, one would not observe a discontinuity in the k_f vs. $E_T(30)$ curve.

Table II. Transition Moments for Aminosulfonates

Solvents	$\lvert\bar{\mu}^{el}_{S_1\rightarrow S_0}\rvert$, D		
	2,6-DNS	1,5-DNS	1,5-DNSA
Hexane	2.62	2.62	2.54
Benzene	2.49	2.61	2.62
Dioxane	2.57	2.72	2.58
DMF	2.65	2.58	2.49
DMSO	2.62	2.51	2.55
CH_3CN	2.70	2.60	2.59
2-Propanol	2.60	2.60	2.35
Ethanol	2.62	2.53	2.36
Methanol	2.65	2.41	2.43
Formamide	2.60	2.28	2.44
Water	2.78	2.37	2.37

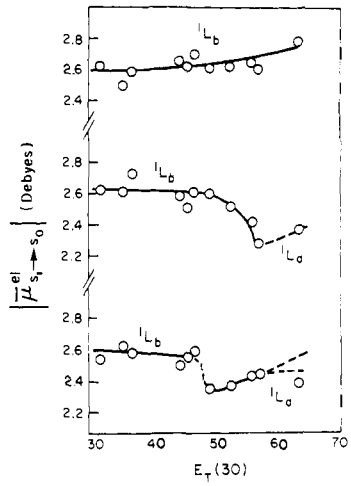

Figure 13. Transition moments as a function of solvent polarity. Top: 2,6-DNS. Middle: 1,5-DNS. Bottom: 1,5-DNSA.

It should be possible to correlate the transition moment for 1,5-DNS and derivatives $|\bar{\mu}^{el}_{S_1\rightarrow S_0}|$ with measured k_f values, via the Einstein spontaneous emission coefficient A_{21}:

$$\frac{1}{\tau_0} = k_f = A_{21} = \frac{64\pi^4}{3h} n^2 \bar{\nu}_f^{\,3} \left| \bar{\mu}^{el}_{S_1\rightarrow S_0} \right|^2$$

where n is the index of refraction, h is Planck's constant, $\bar{\nu}_f$ is the mean frequency of the fluorescence spectrum. The calculated values of $|\bar{\mu}^{el}_{S_1\rightarrow S_0}|$ are shown in Table II and are plotted vs. $E_T(30)$ value for 2,6-DNS, 1,5-DNS, and 1,5-DNSA in Figure 13.

In "nonpolar" solvents, $E_T(30) < 45$, the $|\bar{\mu}|$ values of these three compounds are all about equal, approximately 2.6 D. This result indicates that the emitting state of all three compounds in nonpolar solvents is the ^1L_b state. As the solvent polarity increases, the $|\bar{\mu}|$ value of 2,6-DNS increases slightly in a continuous fashion. This supports the idea that the emitting state of 2,6-DNS is the same in both polar and nonpolar solvents.

The magnitudes of $|\bar{\mu}|$ for 1,5-DNS and 1,5-DNSA decrease slightly with increasing solvent polarity and then both drop abruptly at $E_T(30) \simeq 50$. The minimum value of $|\bar{\mu}|$ for 1,5-DNS occurs at $E_T(30) \simeq 56$ and for 1,5-DNSA at $E_T(30) \simeq 50$. Such a discontinuity of $|\bar{\mu}|$ values for 1,5-DNS and 1,5-DNSA constitutes strong evidence that inversion of excited states takes place in polar solvents.

The results shown in Figure 13 indicate a lower dipole moment for the ^1L_a state than for ^1L_b. One should bear in mind that the so-called ^1L_a transition is no longer a strong $\pi \rightarrow \pi^*$ transition; the large amount of charge-transfer character has reduced its transition moment, and thus $\bar{\mu}(^1L_a) < \bar{\mu}(^1L_b)$ is reasonable in this particular case. The ^1L_a state is also strongly solvent sensitive, and its $|\bar{\mu}|$ value increases with solvent polarity after the inversion; hence there is no doubt that ^1L_a of 1,5-DNS is a polar state.

In Figure 13, most of those points which deviate from the curves are for solvents where solubility problems were encountered. Error arises from measurement of k_f and $\bar{\nu}_f$ since these values are extrapolated instead of being measured directly. For instance, 1,5-DNSA has low solubility in water; the measurements of ϕ_f, τ_f, and $\bar{\nu}_f$ were done by extrapolating from water–ethanol mixtures; the very low value of ϕ_f and τ_f also will cause a high percentage of error, which will be multiplied in the calculation of $|\bar{\mu}|$.

Calculated values of $|\bar{\mu}^{el}_{S_1 \rightarrow S_0}|/e$ values of 2,6-DNS range from 0.54 Å in nonpolar solvents to 0.57 Å in water. Unfortunately there is no direct comparison with Brand's $|\bar{M}^{el}_{S_1 \leftarrow S_0}|/e$ value,[13] however, by estimating this value,[13] it should be about 0.40 Å. Therefore, because $|\bar{\mu}^{el}_{S_1 \rightarrow S_0}|/e$ is greater than $|\bar{\mu}^{el}_{S_1 \leftarrow S_0}|/e$, the excited-state dipole moment is indeed larger than that of the ground state. The calculated $|\bar{\mu}^{el}_{S_1 \rightarrow S_0}|/e$ for 1,5-DNS is 0.54 Å for ^1L_b and 0.48 Å for ^1L_a.

Acknowledgments. We thank L. Brand for the gift of 2,6-DNS; Leon N. Klatt for help in the computer-simulated studies; Shirley Springs for some measurements; A. Weller for helpful discussions; J. D. Winefordner and J. Mousa for phosphorescence measurements; Shirley Hercules for her assistance in writing the manuscript. One of us (Y.-H.L.) thanks the U.S. Public Health Service for a postdoctoral fellowship. This work was supported by the National Institutes of General Medical Sciences under Grant GM-17913.

References and Notes

(1) (a) This work was supported in part by the National Institutes of General Medical Sciences under Grant GM-17913; (b) U.S. Public Health Postdoctoral Fellow, 1972–1973; (c) Department of Entomology.
(2) (a) L. Stryer, *J. Mol. Biol.*, **13**, 482 (1965); (b) W. O. McClure and G. M. Edelman, *Biochemistry*, **5**, 1908–1919 (1966); **6**, 559–566 (1967); **6**, 567–572 (1967).
(3) R. F. Chen and J. C. Kernohan, *J. Biol. Chem.*, **242**, 5813–5823 (1967).
(4) L. Stryer, *Science*, **162**, 526–533 (1968).
(5) G. M. Edelman and W. O. McClure, *Acc. Chem. Res.*, **1**, 65 (1968).
(6) C. M. Himel, R. T. Mayer, and L. L. Cook, *J. Polym. Sci., Part A-1*, **8**, 2219–2230 (1970).
(7) S. K. Chakrabarti and W. R. Ware, *J. Chem. Phys.*, **55**, 5494 (1971).
(8) L. Brand and J. R. Gohlke, *J. Biol. Chem.*, **246**, 2317 (1971).
(9) C. J. Seliskar and L. Brand, *J. Am. Chem. Soc.*, **93**, 5414 (1971).
(10) D. C. Turner and L. Brand, *Biochemistry*, **7**, 3381 (1968).
(11) C. J. Seliskar and L. Brand, *Science*, **171**, 799 (1971).
(12) M. Godfry and J. N. Murrell, *Proc. R. Soc. London, Ser. A*, **278**, 57 (1964); **278**, 64, 71 (1964).
(13) C. J. Seliskar and L. Brand, *J. Am. Chem. Soc.*, **93**, 5405 (1971).
(14) K. Nishimoto and R. Fujishiro, *Bull. Chem. Soc. Jpn.*, **37**, 1660 (1964).
(15) K. Nishimoto, *Bull. Chem. Soc. Jpn.*, **39**, 645 (1966).
(16) V. Fussgänger, *Ber.*, **35**, 976 (1902).
(17) D. J. R. Laurence, *Methods Enzymol.*, **4**, 174 (1957).
(18) R. F. Chen, *Nature (London)*, **209**, 69 (1966).
(19) C. M. Himel and R. T. Mayer, *Anal. Chem.*, **42**, 130 (1970).
(20) A. N. Fletcher, *J. Mol. Spectrosc.*, **23**, 22 (1967).
(21) E. T. Mesewc, "Excited States of Proteins and Nucleic Acids", R. F. Steiner and I. Weinryb, Ed., Plenum Press, New York, N.Y., 1971, p 57.
(22) E. M. Kosower, *J. Am. Chem. Soc.*, **80**, 3253 (1958).
(23) K. Dimroth, C. Reichert, T. Siermann, and F. Bohlmann, *Justus Liebigs Ann. Chem.*, **861**, 1 (1963).
(24) E. M. Kosower and K. Tanizawa, *Chem. Phys. Lett.*, **16**, 419 (1972).
(25) L. Stryer, *J. Am. Chem. Soc.*, **88**, 5708 (1966).
(26) J. R. Platt, *J. Chem. Phys.*, **17**, 484 (1949).
(27) J. N. Murrell, "The Theory of the Electronic Spectra of Organic Molecules", Wiley, New York, N.Y., 1963, Chapter 6.
(28) M. Kasha and H. R. Rawls, *Photochem. Photobiol.*, **7**, 561 (1968).
(29) N. Mataga, *Bull. Chem. Soc. Jpn.*, **36**, 654 (1963).
(30) M. A. El-Bayonmi, J. P. Dalle, and M. F. O'Duyer, *J. Am. Chem. Soc.*, **92**, 3494 (1970).
(31) S. G. Schulman and A. C. Capomacchia, *Spectrochim. Acta, Part A*, **28**, 1 (1972).
(32) R. M. Hochstrasser and C. J. Marzzacco in "Luminescence", E. C. Lim, Ed., W. A. Benjamin, New York, N.Y., 1969, pp 631–656.

Optically Active Amines. XVIII.[1] Spectral Observations on Optically Active N-Substituted Pyrroles

Howard E. Smith,*[2a] Richard K. Orr,[2a,3] and Fu-Ming Chen[2b]

Contribution from the Department of Chemistry, Vanderbilt University, Nashville, Tennessee 37235, and the Department of Chemistry, Tennessee State University, Nashville, Tennessee 37203. *Received September 3, 1974*

Abstract: The CD spectra of (*R*)-1-(1,2,2-trimethylpropyl)pyrrole [(*R*)-**1**] and (*S*)-1-(1-phenylethyl)pyrrole [(*S*)-**2**] in hexane give evidence for the existence of a weak electronic transition of pyrrole between 230 and 240 nm which in the uv (isotropic absorption) spectrum is usually hidden under the tail of the more intense absorption band around 210 nm. The uv spectrum of (*R*)-**1** shows a maximum at 216 nm (ϵ 6400) and a shoulder near 202 nm (ϵ 4400). The CD spectrum displays a weak maximum at 236 nm ([θ] −670), a shoulder near 215 nm ([θ] −8300), and a strong maximum at 200 nm ([θ] −17,000). The Cotton effect at 236 nm is intensified by a phenyl substituent, and (*S*)-**2** shows a very intense maximum at 238 nm ([θ] +11,000). Based on the CD observations in conjunction with CNDO/S calculations, the 236- and 216-nm bands of the 1-pyrryl chromophore are assigned as $A_1 \leftarrow A_1$ and $B_2 \leftarrow A_1$ transitions of pyrrole, respectively, and the shoulder at 200 nm to the $B_1 \leftarrow A_1$ and $A_2 \leftarrow A_1$ transitions.

Until recently it was generally accepted that the uv (isotropic absorption) spectrum of pyrrole in hexane consists of a strong band in the vicinity of 210 nm (ϵ 5100) and a less distinct band near 240 nm (ϵ 300).[4] However, it has been demonstrated with highly purified pyrrole that the long wavelength band in earlier measurements was the result of impurity.[5] Our purpose now is to present evidence from the CD spectra of chiral N-substituted pyrroles for the existence of a weak electronic transition of pyrrole between 230 and 240 nm[6] which in the uv spectrum in hexane is usually hidden under the tail of the more intense band around 210 nm.[7] On the basis of the CD observations in conjunction with CNDO/S calculations, we also assign this weak electronic transition as well as the other transitions responsible